

# Theoretical Modeling of Enzyme Reaction Chemistry: The Electron Transfer of the Reduction Mechanism in CuZn Superoxide Dismutase

Maira D'Alessandro,<sup>†</sup> Massimiliano Aschi,<sup>\*‡</sup> Maurizio Paci,<sup>†</sup> Alfredo Di Nola,<sup>§</sup> and Andrea Amadei<sup>\*‡</sup>

Dipartimento di Scienze e Tecnologie Chimiche, Università di Roma "Tor Vergata", via della Ricerca Scientifica 1, 00133 Roma, Italy, Dipartimento di Chimica, Ingegneria Chimica e Materiali, Università degli studi dell'Aquila, via Vetoio, 67010 L'Aquila, Italy, and Dipartimento di Chimica, Università di Roma "La Sapienza", P. le Aldo Moro 5, 00185 Roma, Italy

Received: March 18, 2004; In Final Form: June 21, 2004

In this paper, we investigate the first step of the copper–zinc superoxide dismutase enzymatic cycle, involving the binding of a superoxide anion, the transfer of one electron toward the copper, and the simultaneous detachment of His63. By means of combining the perturbed matrix method (PMM) [*Chem. Phys. Lett.* **2001**, 365, 450–456] with basic statistical mechanical relations, presented in the accompanying paper, we describe the coupling between these chemical events and the atomic motions of the complex environment of the reaction center. Results clearly show that the protein–solvent environment fluctuations are essential to understand the reaction mechanism which is based on the concerted rupture of the copper–histidine coordination bond and the copper–superoxide bond in the active site.

## Introduction

Copper–zinc superoxide dismutase (CuZnSOD) is a homodimeric protein<sup>1–3</sup> which catalyzes the superoxide anion ( $\text{O}_2^-$ ) disproportionation.



Each subunit contains one copper (Cu) and one zinc (Zn) atom. The Cu is coordinated to four histidines forming a distorted square planar geometry.<sup>2</sup> One of these histidines (His63) formally exhibits a negative charge and acts as a bridge between Cu and Zn.<sup>3</sup> The role of these atoms is known to be substantially different. The Zn atom does not directly participate to the catalytic process and has a structural stabilization role,<sup>3</sup> while Cu plays an essential role in the enzymatic catalysis.<sup>1</sup> Understanding the details of the catalytic mechanism of CuZnSOD has been for a long time,<sup>1,3–8,10,11</sup> and still is<sup>9,12</sup> at the center of a very active interest. In this respect different plausible mechanisms have been proposed. According to the most widely accepted,<sup>1,3–9</sup> in the first step (1) of the reaction the  $\text{O}_2^-$  is oxidized by  $\text{Cu}^{2+}$  to molecular oxygen ( $\text{O}_2$ ). Subsequently (2), a second superoxide anion is reduced by  $\text{Cu}^+$  to produce hydrogen peroxide. In this mechanistic scheme,<sup>9</sup> one of the crucial points is the breaking down of the coordination bond between the  $\text{Cu}^+$  and the nitrogen of the His63 imidazole, just coincident with the superoxide oxidation. An alternative picture<sup>10,11</sup> has suggested that the superoxide anion and  $\text{Cu}^{2+}$  may form a stable intermediate state which, therefore, oxidizes a second superoxide molecule. In this second mechanistic scheme, the rupture of the bond between Cu and His63 does not need

to occur at all. This last mechanism has been recently experimentally ruled out<sup>13–16</sup> confirming the occurrence of the first hypothesis. The great difficulty in understanding the CuZnSOD reaction mechanism, as for any enzymatic reaction, is due to the chemical complexity of the reaction steps involved and their coupling with the atomic and molecular motions which influence and modulate the reactivity. We have addressed this problem with the use of a theoretical–computational approach (described in the preceding paper presented in this issue<sup>17</sup>), based on the combination of the recently proposed perturbed matrix method (PMM)<sup>18,19</sup> with basic statistical mechanics for calculating the reaction free energy surface and related electronic properties in complex molecular systems. The main feature of PMM is the capability of treating the electronic properties by means of quantum mechanical first principles and molecular simulations and proved to be rather efficient for reproducing the UV–vis spectroscopical signals of a variety of systems ranging from small molecules<sup>21</sup> to biomacromolecules<sup>20,22</sup> in solution. In this paper, we report the chemical description of the first step of the enzymatic reaction of CuZnSOD: the  $\text{O}_2^-$ – $\text{Cu}^{2+}$  binding event, the following electron transfer, and  $\text{Cu}^+$ –His63 bond breaking.

## Methods

In the first step of the present study we carried out a classical molecular dynamics (MD) simulation of human dimeric CuZnSOD with  $\text{O}_2^-$  bound to the Cu, at one of the two active sites of the enzyme. Since no crystallographic wild-type structure is available, we used for the simulation the structure of a crystallized mutant (PDB code: 1SPD<sup>23</sup>) with the biochemical activity considered equivalent to the wild-type one.<sup>24,25</sup> Moreover, in the absence of the structure of the  $\text{O}_2^-$ –CuZnSOD complex, we used for modeling the Cu superoxide core, an available structure of bovine CuZnSOD complexed with an azido group (PDB code: 1SXZ<sup>26</sup>) which was substituted in our simulation with  $\text{O}_2^-$ . The charges of the active site (composed

\* To whom the correspondence should be addressed.

<sup>†</sup> Università di Roma "Tor Vergata".

<sup>‡</sup> Università degli studi dell'Aquila.

<sup>§</sup> Università di Roma "La Sapienza".

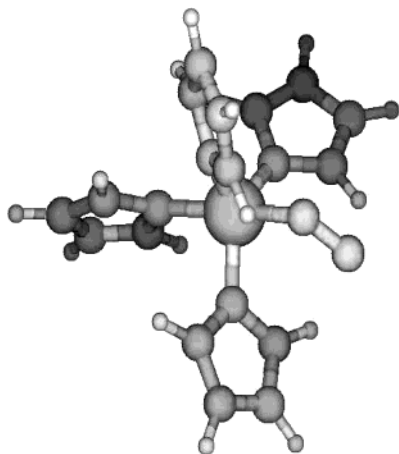


**Figure 1.** Picture of the quantum center (CHS) we used for quantum chemical and PMM calculations.

by Zn, Cu,  $O_2^-$ , by the four imidazoles of the copper coordinating histidines, by the two imidazoles of the zinc coordinating histidines, and by the zinc coordinating aspartate) were reevaluated through quantum chemical calculations using a density functional theory-based approach. Such atomic charges were used in the MD simulation. In particular the Kohn–Sham orbitals of the above structure were optimized using the hybrid B3LYP functional<sup>27,28</sup> in conjunction with a 3-21G atomic basis set.<sup>29</sup> These orbitals were then used for evaluating the point charges adopting the CHelpG protocol.<sup>30</sup> All the other elements of the force field were taken from the GROMOS96 force field.<sup>31</sup> The molecule was immersed in a rectangular box with sides aligned along its principal axis, filled with 10372 spc water molecules<sup>32</sup> and nine sodium ions in order to retain the charge neutrality. After an energy minimization and a dynamical relaxation of the system, the productive run was carried out in *NVT* ensemble for 14 ns. The time step was 2 fs, and the temperature was kept constant at 300 K by the isoGaussian algorithm.<sup>33</sup> Periodic boundary conditions were systematically applied and long-range interactions were treated using the particle-mesh Ewald method<sup>34</sup> with the fourth order cubic interpolation. Nonbonded short-range interactions were evaluated within 0.9 nm cutoff radius. The algorithm SHAKE<sup>35</sup> was used to constrain bond lengths and the roto-translational constraint of the solute<sup>36</sup> was also adopted in the simulation. The parallel version of the GROMACS package was used for obtaining the trajectory, and it was also used with a certain number of our own routines for analyzing the trajectory.

The application of PMM can be carried out provided that a rather reliable description of the unperturbed, i.e., in vacuo, quantum center is available. In this study we defined as quantum center the  $His_4CuO_2^-$  (CHS) complex (Figure 1), where in order to increase the level of the quantum chemical calculations the Zn was replaced by a proton. This choice, which at a first sight could appear rather questionable, can be justified by the presence in the literature of previous theoretical studies in which the same approximation has been successfully adopted for simulating the CuZnSOD reaction<sup>12</sup> and related equilibrium properties.<sup>37</sup> First of all we optimized the geometry of CHS using the B3LYP functional and the 3-21G basis set for all the atoms with the exception of the  $O_2^-$  and copper, for which the more extended 6-311+g(d) basis set<sup>38,39</sup> was adopted. Therefore, starting from the absolute potential energy minimum, we selected three main internal coordinates (reaction coordinates): the Cu– $O_2^-$ , His63–Cu, and His120–Cu (His120 is one of the other three copper coordinating histidines) distances. The rest of CHS was kept

frozen in its absolute energy minimum geometry. We wish herein to remark that the level of quantum chemical calculations used to describe the unperturbed CHS was selected because of its capability of including, with a relatively low computational cost, the electron dynamical correlation, which is very important where a chemical process is concerned. Moreover, it had already been applied in the past with good results on molecular systems containing one or more Cu atoms.<sup>44,46–51</sup> With this procedure we calculated the ground unperturbed reaction surface for the  $Cu^{2+}-O_2^-$  covalent binding and for the initial His–Cu bonds rupture. In correspondence of each of such configurations, we subsequently carried out configuration interaction calculations<sup>41</sup> with all the single and double excitations (CISD) for describing the unperturbed excited states. The B3LYP vectors, and not the usual Hartree–Fock (HF) ones, were utilized for this purpose. We adopted this computational scheme on the basis of a preliminary calibration of the method carried out on a series of model biomimetic inorganic systems,<sup>40</sup> structurally rather close to the CuZnSOD active site, for which we tried to reproduce the UV maximum absorption. The B3LYP–CISD calculations provided better results than the HF–CISD ones. The ground and the first seven excited states were therefore taken into account for building the perturbed Hamiltonian matrix to be used in PMM as described in the accompanying paper. Briefly, the perturbed Hamiltonian matrix  $\tilde{H}$  of the quantum center on the Born–Oppenheimer (BO) surface is

$$\tilde{H} \cong \tilde{H}^0 + q_T \mathcal{V} \tilde{I} + \tilde{Z}_1 + \Delta \tilde{V} \quad (3)$$

where  $\tilde{H}^0$  is the unperturbed Hamiltonian matrix of the quantum center constructed via the CISD calculations including the ground-state plus seven excited states,  $q_T$  is the total charge of the quantum center,  $\mathcal{V}$  is the perturbation electric potential exerted by the environment on the quantum center,  $\tilde{Z}_1$  is the perturbation matrix provided by the inner products between the unperturbed transition dipoles and the perturbing electric field, and  $\Delta \tilde{V}$  approximates the perturbation due to all the terms from the quadrupoles on, as a simple short-range potential. It is worth to note that at each MD frame the electric potential and field exerted by the environment can be calculated and the perturbed Hamiltonian matrix diagonalized. Hence a trajectory of the perturbed eigenvalues and eigenvectors is obtained. Such a calculation, if carried out along predefined reaction coordinates, provides the free energy change ( $\Delta A$ ) and the related electronic properties ( $\langle \chi_b \rangle_b$ ) at a generic point  $\eta_b$  of the reaction coordinates<sup>17</sup>

$$\Delta A \cong -kT \ln \langle e^{-\beta \Delta(\epsilon' + q_T \mathcal{V})} \rangle_{\eta_a}^0 \quad (4)$$

$$\langle \chi_b \rangle_b \cong \frac{\langle e^{-\beta \Delta(\epsilon' + q_T \mathcal{V})} \chi_b \rangle_{\eta_a}^0}{\langle e^{-\beta \Delta(\epsilon' + q_T \mathcal{V})} \rangle_{\eta_a}^0} \quad (5)$$

In the previous equations  $\epsilon'$  is the eigenvalue of the perturbation matrix  $\tilde{Z}_1$ ,  $\Delta(\epsilon' + q_T \mathcal{V})$  provides the energy change, for each MD frame, due to the transition along the reaction coordinates, and  $\eta_a$  is the position of the reaction coordinates used to obtain the statistical ensemble, i.e., used in the MD simulation. Moreover, the subscript  $\eta_a$  and the zero superscript of the averaging operator means that the average is taken in the statistical ensemble where the reaction coordinates are fixed at  $\eta_a$  with the quantum center in its ground vibrational state. Note that the use of a frozen quantum center, except for the explicit reaction coordinates considered, is not at all required by our approach<sup>17,19</sup> but allows for a simple and reliable PMM

application when we deal with rigid or semirigid quantum centers. The perturbing electric field, used to construct the perturbed Hamiltonian matrix utilized in PMM, was obtained at each MD configuration by the atomic charges within the simulation box (excluding CHS charges). The above procedure was carried out for both the triplet and for the singlet magnetic states. To investigate the relation of the reaction free energy surface and related electronic properties with the conformational transition of the enzyme, we evaluated them as a function of the generalized conformational coordinates provided by the essential dynamics analysis on C- $\alpha$  motions.<sup>20,43</sup> All the quantum chemical calculations for the unperturbed system (isolated CHS), were done using the Gamess package.<sup>42</sup>

## Results and Discussion

In the first part of our investigation, we focused our attention on the structural and dynamical features of CuZnSOD. For this purpose a 14 ns MD simulation was carried out. The time course of the root-mean-square deviation (RMSD) of the C- $\alpha$  atoms with respect to the initial structure shows that within 4 ns a stable RMSD of 0.2 nm is reached, indicating that the system is equilibrated. This is the necessary condition for evaluating whatever property including, like in the present case, the free energy surface associated with the electron transfer. The small RMSD suggests that at least with the presently employed force field, CuZnSOD in water at 300 K does not undergo dramatic structural changes. The MD trajectory also revealed that CHS has a rather rigid structure which, as mentioned in our previous articles,<sup>20–22</sup> represents a necessary condition for a straightforward application of PMM.

As described in the methodological section, B3LYP calculations were used for obtaining the unperturbed binding reaction surface starting from the energy minimum of the CHS complex and changing the Cu–O<sub>2</sub><sup>−</sup> distance, in the range 1.8–2.6 Å. Such a minimum, obtained by fully optimizing the structure on the triplet surface, shows a Cu–O<sub>2</sub><sup>−</sup> distance equal to 1.995 Å in good agreement with Parrinello's results.<sup>12</sup> Note that within our approximation<sup>17,21</sup> the potential energy and free energy reaction surfaces are identical for the unperturbed condition. We wish to remark that, although investigated, the singlet surface will not be outlined in this paper as it is systematically energetically much higher than the triplet and therefore not important when a thermal reaction is concerned. From the analysis of the B3LYP results it emerges, as expected,<sup>12</sup> that the electron transfer does not occur at any position of the unperturbed binding reaction surface. In fact, when the Cu–O<sub>2</sub><sup>−</sup> distance decreases from 2.6 to 1.995 Å, an energy variation larger than 70 kJ/mol is observed, but no electron flux toward copper is present (the total Mulliken charge of the superoxide ion, in electron units, remains basically about −0.6, and only a slight electron flux toward superoxide is observed). From our calculations, it turned out that the chemical bond between superoxide ion and copper is mainly due to the overlap of the d<sub>xy</sub> orbital of Cu<sup>2+</sup>, containing the unpaired electron, with the singly occupied O<sub>2</sub><sup>−</sup> antibonding  $\pi^*$  orbital. The O<sub>2</sub><sup>−</sup> lone pair, on the other hand, remains in the symmetry unfavored  $\pi^*$  orbital. Moreover within the sampled reaction surface, the spin density at the nuclei does not undergo significant changes, remaining essentially around 0.6 au on the O<sub>2</sub><sup>−</sup> and 0.75 au on the Cu. Interestingly, the analysis of the DFT/CISD excited states reveals that the first excitation, requiring 45 kJ/mol at the minimum (free) energy position, essentially describes one electron "jumping" from the O<sub>2</sub><sup>−</sup> to an antibonding orbital mainly associated with Cu and His63, providing the electron

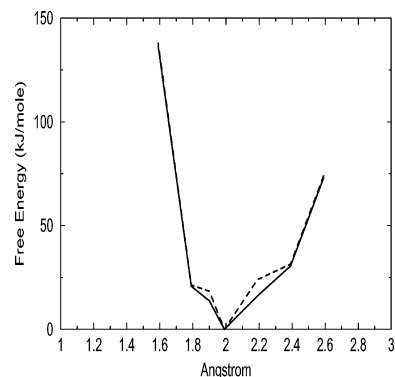


**Figure 2.** Cu–O<sub>2</sub><sup>−</sup> binding free energy reaction surface for the unperturbed (dashed line) and perturbed (solid line) CHS, as a function of the Cu–O distance.

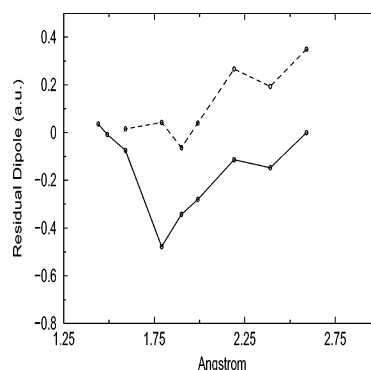


**Figure 3.** Residual dipole along Cu–O<sub>2</sub><sup>−</sup> chemical bond for the unperturbed (dashed line) and perturbed (solid line) CHS as a function of Cu–O distance.

transfer in vacuo. However, the relevant energy involved in the excitation makes such a process basically forbidden at 300 K. To study the reaction mechanism in the enzyme, including the whole protein, the solvent and the effects of conformational fluctuations, we considered two chemical processes: the Cu–O<sub>2</sub><sup>−</sup> binding and the concerted breaking of the histidines–Cu and Cu–O<sub>2</sub><sup>−</sup> bonds. In Figure 2, we show the free energy reaction surface for Cu–O<sub>2</sub><sup>−</sup> binding in vacuo (unperturbed) and within the solvated protein (perturbed). From the figure it is clear that, for this reaction step, the interaction between CHS and the fluctuating environment does not significantly change the corresponding reaction surface.

In Figure 3, we also show, for the unperturbed and the perturbed conditions, the residual dipole along the Cu–O<sub>2</sub><sup>−</sup> chemical bond for the same reaction path. This observable describes the changes of electron density in the direction of the Cu–O<sub>2</sub><sup>−</sup> chemical bond, and it is obtained via

$$\Delta\mu = (\mu - \mu_{\text{ref}}) \cdot \mathbf{b} \quad (6)$$

where  $\mu$  is the actual electric dipole at a given position of the reaction coordinate as obtained by quantum chemical and PMM<sup>21</sup> calculations,  $\mu_{\text{ref}}$  is the dipole at the same position of the reaction coordinate obtained using the unperturbed charge density at a reference Cu–O<sub>2</sub><sup>−</sup> distance (2.6 Å) and  $\mathbf{b}$  is the unit vector defining the Cu–O<sub>2</sub><sup>−</sup> chemical bond direction. Hence  $\Delta\mu$  provides a direct measure of the nontrivial charge density modification involved in the electron transfer, obtained with respect to the unperturbed reference charge distribution (−0.6 au for the superoxide ion):  $\Delta\mu < 0$  implies a negative-charge flux toward the superoxide while  $\Delta\mu > 0$  provides a negative-charge flux toward the copper.

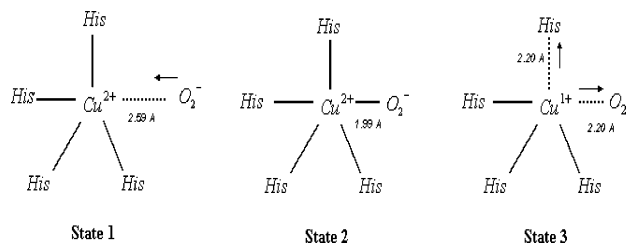


**Figure 4.** Schematic view of the three chemical states.

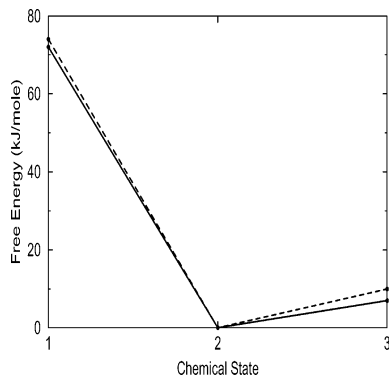


**Figure 5.** Three states free energy surface for the reaction involving His120-Cu bond rupture: unperturbed CHS = dashed line; perturbed CHS = solid line.

This figure shows that, as the superoxide approaches the copper, a slight electron flux toward the  $O_2^-$  moiety is present ( $\Delta\mu < 0$  and/or decreasing), although in the perturbed condition at a lower extent. Interestingly, the perturbed curve is always higher, indicating that the protein environment stabilizes a superoxide ion with a lower absolute total charge. However, the perturbation of the environment does not significantly alter the reaction behavior. Therefore, in agreement with previous papers,<sup>10–12</sup> the electron transfer, along this reaction coordinate, does not occur even in the presence of the proper atomic environment.

To identify the possible reaction path providing the electron transfer, we made the same calculations for the reaction defined by the change of the histidine-Cu and Cu- $O_2^-$  bond distances. We essentially investigated, as a simple reaction path, the early steps of histidine (His63 and His120) -Cu and Cu- $O_2^-$  bond ruptures. We have then schematized the complete reaction surface studied into three chemical states (see Figure 4): Cu- $O_2^-$  bond heavily stretched (2.6 Å, state 1), CHS in the Cu- $O_2^-$  binding minimum free energy condition (Cu- $O_2^-$  bond at 1.995 Å, state 2), and Cu- $O_2^-$  and histidine-Cu bonds initially stretched (both at 2.2 Å, state 3).

The results, for the reaction involving His120-Cu bond rupture (for the perturbed and unperturbed conditions), are shown in Figures 5 (free energy) and 6 ( $\Delta\mu$ ). It is clear that the interaction of CHS with its molecular environment does not provide any relevant effect and hence, like in the unperturbed condition, no electron transfer is present. On the other hand, by inspecting the results for the reaction involving the His63-Cu bond, we do observe a dramatic effect of the protein and solvent interactions on CHS free energy surface (Figure 7) and residual dipole (Figure 8), clearly showing that the electron transfer occurs only in the perturbed CHS. Moreover, the remarkable negative free energy change coupled to the electron transfer, due to the concerted Cu- $O_2^-$  and His63-Cu bonds stretching, implies that such a reaction proceeds spontaneously at high speed. Note that from Figure 8 in the chemical state 3 the residual dipole provides (considering that only copper and

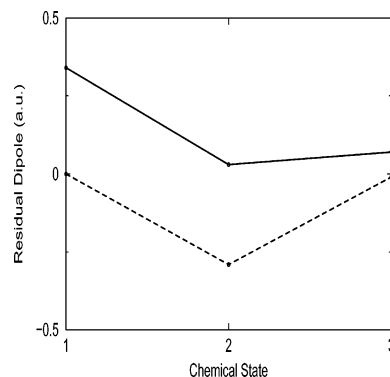


**Figure 6.** Three states residual dipoles along Cu- $O_2^-$  bond for the reaction involving His120-Cu bond rupture: unperturbed CHS = dashed line; perturbed CHS = solid line.

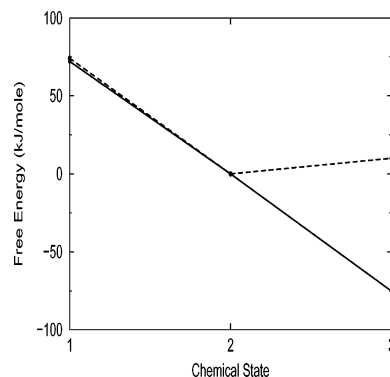


**Figure 7.** Three states free energy reaction surface for the reaction involving His63-Cu bond rupture: unperturbed CHS = dashed line; perturbed CHS = solid line.

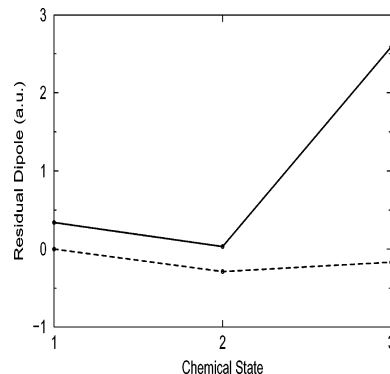


**Figure 8.** Three states residual dipoles along Cu- $O_2^-$  bond for the reaction involving His63-Cu bond rupture: unperturbed CHS = dashed line; perturbed CHS = solid line.

superoxide change their charges from the reference values) an electron transfer of about 0.6 electrons, remarkably corresponding to the reference charge of the superoxide.

The results presented show that the protein-solvent environment exerts a dramatic effect on the chemical reactivity of CHS, inducing and thermodynamically stabilizing the electron-transfer reaction which, on the other hand, cannot take place in the isolated CHS. Moreover, the free energy change for the concerted Cu- $O_2^-$  and His63-Cu bond disruptions implies that the reaction mechanism of the electron transfer is based on their simultaneous breaking (stretch of the His63-Cu bond only, which does not provide electron transfer and is associated with an almost zero free energy change). These results explain the remarkable efficiency of the enzyme activity, based on a reaction mechanism essentially defined by two chemical steps: first a large free energy decrease drives  $O_2^-$  to bind Cu with no

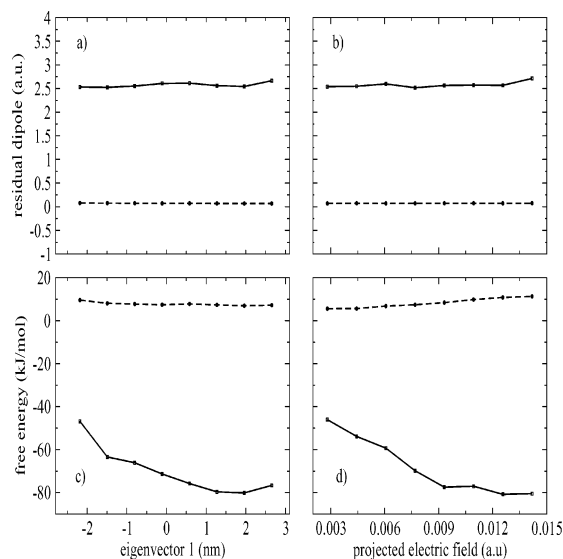


**Figure 9.** Free energy difference for chemical state 2 to chemical state 3 transition (panels c, d) and residual dipole along Cu–O<sub>2</sub><sup>−</sup> bond in chemical state 3 (panels a, b), as a function of (left) the position along the first C-α eigenvector and (right) the perturbing electric field along Cu–O<sub>2</sub><sup>−</sup> bond: solid line corresponds to the stretched His63–Cu bond; dashed line corresponds to the stretched His120–Cu bond.

electron-transfer involved, and subsequently, a second even larger negative free energy change forces the electron transfer via the concerted Cu–O<sub>2</sub><sup>−</sup> and His63–Cu bond ruptures. This reaction mechanism explains well the experimentally observed diffusion rate-limiting step,<sup>5</sup> evidenced in our calculations by the absence of any transition state and actually suggests that this reaction can be considered as an effective concerted chemical process.

To investigate explicitly the relation of such a reaction path with protein conformational fluctuations, we calculated the free energy change upon these bonds stretching (with respect to their equilibrium binding conditions) and the final residual dipole (at chemical state 3) as a function of both the perturbing electric field projected onto the Cu–O<sub>2</sub><sup>−</sup> chemical bond and the position along the first C-α eigenvector, describing the main conformational fluctuation of the backbone, as obtained by essential dynamics analysis<sup>20,43</sup> (see Figure 9). From the figure it is evident that the main protein backbone conformational fluctuation as well as the projected perturbing electric field, significantly modulates the thermodynamics of the Cu–O<sub>2</sub><sup>−</sup> and His63–Cu bonds stretching (free energy variation up to 35 kJ/mol), although the free energy change (panels c,d) remains largely negative in the whole accessible conformational space. Interestingly, the electron transfer is essentially present at all the accessible conformations of the chemical state 3 (panels a,b). Note that the projected electric field, as obtained by the MD simulation, is always positive, hence pushing electrons from O<sub>2</sub><sup>−</sup> to Cu. On the other hand from the same figure it turns out that protein fluctuations do not modify the free energy profile and the residual dipole for the Cu–O<sub>2</sub><sup>−</sup> and His120–Cu bonds stretching which remains chemically unproductive and thermodynamically unfavored in the whole accessible conformational space.

Finally, as evidenced by the previous results, the perturbing electric field, projected onto the Cu–O<sub>2</sub><sup>−</sup> bond, is the main responsible of the enzymatic activity, and hence, its decomposition into the residue contributions directly provides the relevance of each residue for the catalytic process. Asp 83, Arg 124, Glu 133, Asp 125, Glu 132, Arg 115, and Arg 143 provide the largest

positive average electric fields projected along the Cu–O<sub>2</sub><sup>−</sup> bond, hence favoring the electron transfer. On the other hand Lys 128, His 71, and Lys 136 are clearly inhibitors of the reaction as they are associated with large negative average projected fields. Interestingly, most of such residues present also the largest field fluctuations suggesting that their effect on CHS is exerted not only as a static one but also as a pattern of relatively large field fluctuations. It is worth to note that in previous literature<sup>10–12</sup> the active site proximal arginine (in our case Arg 143) was assumed to inhibit the electron transfer on the basis of the in vacuo quantum chemical calculations, where such a residue was modeled by an ammonium ion fixed at the corresponding crystal position of the uncomplexed (bovine) SOD. Our results clearly show that the proximal arginine, when treated within the explicit fluctuating protein–solvent system and in the presence of the ligand bound, considerably favors the electron transfer step via its perturbing electric field. Note also that, as expected, only the residues of the subunit where the Cu–O<sub>2</sub><sup>−</sup> complex is present influence significantly the chemical process and the solvent, although showing a rather small average perturbing field and corresponding standard deviation, provides a nonnegligible effect.

## Conclusions

In this paper, we studied the superoxide anion binding and subsequent Cu<sup>2+</sup> reduction representing the chemical processes of the first step of CuZnSOD catalytic cycle. Such a complex reaction, which is of great biochemical interest, has been extensively studied in the last 2 decades, both experimentally and theoretically, but its mechanism was not still completely understood as the theoretical approaches used were not able to describe the essential chemical step involved in this reaction: the electron transfer. By means of combining PMM with statistical mechanical relations, we addressed this problem explicitly modeling the coupling occurring between the reaction center and the atomic and molecular fluctuations of its complex environment (the protein–solvent system). Such perturbative effects, typically neglected in usual quantum chemical calculations, are in the present case absolutely determinant for the occurrence of the electron transfer. From our results clearly emerges the two-step reaction mechanism generally proposed:<sup>1,3–9</sup> first a large free energy decrease drives O<sub>2</sub><sup>−</sup> to bind Cu with no electron-transfer involved, and subsequently, a second even larger negative free energy change forces the electron transfer via the concerted Cu–O<sub>2</sub><sup>−</sup> and His63–Cu bond disruptions. Interestingly, conformational fluctuations, although rather relevant for the free energy associated with the electron transfer reaction step, do not switch off the catalysis in the whole conformational space accessible. The enzyme hence is constructed to provide a well-defined perturbing electric field pattern, resulting in a very high catalytic efficiency. Moreover, the decomposition of the perturbing field in residue contributions revealed the presence of a set of key residues stimulating or inhibiting the reaction process. Finally, such results suggest that the theoretical–computational method used is very promising not only for a basic understanding of biochemical reactions in proteins but also for use as a possible powerful tool to design new drugs and mutants of biological interest.

## References and Notes

- (1) McCord, J. M.; Fridovich, S. J. *J. Biol. Chem.* **1969**, *241*, 6049.
- (2) Tainer, J. A.; Gelzoff, E. D.; Beem, K. F.; Richardson, J. S.; Richardson, D. C. *J. Mol. Biol.* **1982**, *160*, 181–217.
- (3) Strothkamp, K. G.; Lippard, S. J. *Acc. Chem. Res.* **1982**, *15*, 318–326.

- (4) Weinstein, J.; Bielski, B. H. *J. Am. Chem. Soc.* **1980**, *102*, 4916–4919.
- (5) Fee, J. A.; Bull, C. J. *Biol. Chem.* **1986**, *261*, 13000.
- (6) Tainer, J. A.; Getzoff, E. D.; Richardson, J. S.; Richardson, D. C. *Nature (London)* **1983**, *396*, 284.
- (7) Fielden, E. M.; Roberts, P. B.; Bray, R. C.; Lowe, D. J.; Mautner, G. N.; Rotilio, G.; Calabrese, L. *Biochem. J.* **1974**, *139*, 49.
- (8) Klugh Hoth, D.; Fridovich, S. J.; Rabani, J. *J. Am. Chem. Soc.* **1973**, *95*, 2786.
- (9) John Hart, P.; Balbirnie, M. M.; Ogihara, N. L.; Nersissian, A. M.; Weiss, M. S.; Valentine, J. S.; Eisenberg, D. *Biochemistry* **1999**, *38*, 2167–2178.
- (10) Osman, R.; Basch, H. *J. Am. Chem. Soc.* **1984**, *106*, 5710–5714.
- (11) Rosi, M.; Sgamellotti, A.; Tarantelli, F.; Bertini, I.; Luchinat, C. *Inorg. Chem.* **1986**, *25*, 1005.
- (12) Carloni, P.; Blochl, P. E.; Parrinello, M. *J. Phys. Chem.* **1995**, *99*, 1338–1348.
- (13) Bertini, I.; Luchinat, C.; Monnanni, R. *J. Am. Chem. Soc.* **1985**, *107*, 2178–2179.
- (14) Blackburn, N. J.; Hasnain, S. S.; Binsted, N.; Diakun, G. P.; Garner, C. D.; Knowles, P. F. *Biochem. J.* **1984**, *219*, 985–990.
- (15) Ogihara, N. L.; Parge, H. E.; Hart, P. J.; et al. *Biochemistry* **1996**, *35*, 2316–2321.
- (16) Murphy, L. M.; Strange, R. W.; Hasnain, S. S. *Structure* **1997**, *5*, 371–379.
- (17) Amadei, A.; D'Alessandro, M.; Aschi, M. *J. Phys. Chem. B* **2004**, *108*, 16250.
- (18) Aschi, M.; Spezia, R.; Di Nola, A.; Amadei, A. *Chem. Phys. Lett.* **2001**, *344*, 374–380.
- (19) Spezia, R.; Aschi, M.; Di Nola, A.; Amadei, A. *Chem. Phys. Lett.* **2002**, *365*, 450–456.
- (20) Spezia, R.; Aschi, M.; Di Nola, A.; Valentin, M. D.; Carbonera, D.; Amadei, A. *Biophys. J.* **2003**, *84*, 2805–2813.
- (21) Amadei, A.; Zazza, C.; D'Abramo, M.; Aschi, M. *Chem. Phys. Lett.* **2003**, *381*, 187–193.
- (22) Aschi, M.; Zazza, C.; Spezia, R.; Bossa, C.; Di Nola, A.; Paci, M.; Amadei, A. *J. Comput. Chem.* **2004**, *7*, 974.
- (23) Deng, H. X.; Hentati, A.; Tainer, J. A.; Iqbel, Z.; Cayabyab, A.; Hung, W. Y.; Getzoff, E. D.; Hu, P.; et al. *Science* **1993**, *261*, 1047.
- (24) Lepock, J. R.; Frey, H. E.; Hallewell, R. A. *J. Biol. Chem.* **1990**, *265*, 21612–21618.
- (25) Hallewell, R. A.; Imlay, K. C.; Laria, I.; et al. *Biochim. Biophys. Res. Commun.* **1991**, *181*, 474–480.
- (26) Ferraroni, M.; Rypniewski, W. R.; Bruni, B.; Orioli, P.; Mangani, S. *J. Biol. Inorg. Chem.* **1998**, *3*, 411.
- (27) Becke, A. D. *Phys. Rev. A* **1988**, *38*, 3098.
- (28) Lee, C.; Yang, W.; Parr, R. G. *Phys. Rev. A* **1988**, *37*, 785.
- (29) Binkley, J. S.; Pople, J. A.; Hehre, W. J. *J. Am. Chem. Soc.* **1980**, *102*, 939.
- (30) Breneman, C. M.; Wiberg, K. B. *J. Comput. Chem.* **1990**, *11*, 8262.
- (31) van Gunsteren, W. F.; Billeter, S. R.; Eising, A. A.; Hunenberger, P. H.; Kruger, P.; Mark, A. E.; Scott, R. P.; Tironi, I. G. *Biomolecular simulations: the GROMOS96 Manual and User Guide*; Hochschulverlag AG an der ETH Zurich: Zurich, Switzerland, 1996.
- (32) Berendsen, H. J. C.; Postma, J. P. M.; van Gunsteren, W. F.; Hermans, J. Interaction models for water in relation to protein hydration. In *Intermolecular Forces*; Pullman, B., Ed.; Reidel: Dordrecht, The Netherlands, 1981.
- (33) Evans, D. J.; Morriss, G. P. *Statistical Mechanics of Nonequilibrium Liquids*; Academic Press: London, 1990.
- (34) Darden, T. A.; York, D. M.; Pedersen, L. G. *J. Chem. Phys.* **1993**, *98*, 10089.
- (35) Ryckaert, J. P.; Ciccotti, G.; Berendsen, H. J. C. *J. Comput. Phys.* **1977**, *23*, 327.
- (36) Amadei, A.; Chillemi, G.; Ceruso, M. A.; Grottesi, A.; Di Nola, A. *J. Chem. Phys.* **2000**, *112*, 9–23.
- (37) Konecny, R.; Li, J.; Fisher, C. L.; Dillet, V.; Bashford, D.; Noodleman, L. *Inorg. Chem.* **1999**, *38*, 940.
- (38) McLean, A. D.; Chandler, G. S. *J. Chem. Phys.* **1980**, *72*, 5639.
- (39) Raghavachari, K.; Trucks, G. W. *J. Chem. Phys.* **1989**, *91*, 1062.
- (40) Solomon, E. I.; Baldwin, M. J.; Lowery, M. D. *Chem. Rev.* **1992**, *92*, 521.
- (41) Foresman, J. B.; Head-Gordon, M.; Pople, J. A.; Frisch, M. J. *J. Phys. Chem.* **1992**, *96*, 135.
- (42) Schmidt, M. W.; Baldridge, K. K.; Boatz, J. A.; Elbert, S. T.; Gordon, M. S.; Jensen, J. J.; Koseki, S.; Matsunaga, N.; Nguyen, K. A.; Su, S.; Windus, T. L.; Dupuis, M.; Montgomery, J. A. *J. Comput. Chem.* **1993**, *14*, 1347.
- (43) Amadei, A.; Linssen, A. B. M.; Berendsen, H. J. C. *Proteins: Struct., Funct. Gen.* **1993**, *17*, 412–425.
- (44) Olsson, M.H.M.; Ryde, U.; Roos, B. O. *Protein Sci.* **1998**, *12*, 2659–2668.
- (45) Pushie, M. J.; Rauk, A. *Biol. Inorg. Chem.* **2003**, *8*, 53–65.
- (46) Siegbahn, P. E. *Faraday Discuss.* **2003**, *124*, 289–296.
- (47) Blomberg, M. R.; Siegbahn, P. E.; Wikstrom, M. *Inorg. Chem.* **2003**, *42*, 5231–5243.
- (48) Russo, N.; Toscano, M.; Grand, A. *J. Mass Spectrom.* **2003**, *38*, 265–270.
- (49) Martinez, A.; Salcedo, R.; Sansores, L. E.; Medina, G.; Gasque, L. *Inorg. Chem.* **2001**, *40*, 301–306.
- (50) Olsson, M. H.; Ryde, U. *J. Am. Chem. Soc.* **2001**, *123*, 7866–7876.
- (51) Chen, P.; Root, D. E.; Campochiaro, C.; Fujisawa, C.; Solomon, E. I. *J. Am. Chem. Soc.* **2001**, *123*, 7866–7876.